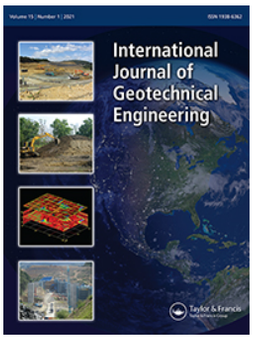

International Journal of Geotechnical Engineering

ISSN: (Print) (Online) Journal homepage: https://www.tandfonline.com/loi/yjge20

Lower bound limit analysis using nonlinear optimization for solving axisymmetric problems using Hoek-Brown yield criterion

Manash Chakraborty & Jyant Kumar

To cite this article: Manash Chakraborty & Jyant Kumar (2021) Lower bound limit analysis using nonlinear optimization for solving axisymmetric problems using Hoek-Brown yield criterion, International Journal of Geotechnical Engineering, 15:1, 28-39, DOI: 10.1080/19386362.2019.1677050

To link to this article: https://doi.org/10.1080/19386362.2019.1677050

INTERNATIONAL JOURNAL OF GEOTECHNICAL ENGINEERING
2021, VOL. 15, NO. 1, 28–39
https://doi.org/10.1080/19386362.2019.1677050

Taylor & Francis
Taylor & Francis Group

TECHNICAL NOTE

Lower bound limit analysis using nonlinear optimization for solving axisymmetric problems using Hoek-Brown yield criterion

Manash Chakraborty[a] and Jyant Kumar[b]

[a]Department of Civil Engineering, Indian Institute of Technology (BHU), Varanasi, India; [b]Department of Civil Engineering, Indian Institute of Science, Bengaluru, India

ABSTRACT

This study presents a computational methodology for solving axisymmetric stability problems in rock mechanics by using the finite element lower bound limit analysis. The *generalized Hoek and Brown* (GHB) yield criterion, which is often recommended to define failure in the intact and jointed rock mass, has been employed. No assumption(s) are required to make either on the value of circumferential stress (σ_θ) or the exponent (α) in the GHB yield expression. It is understood that the assumption of choosing $\alpha = 0.5$ provides an unsafe solution for the values of *GSI* □ 30. For the purpose of illustration, the bearing capacity factor N_σ has been evaluated for a circular footing. The results obtained from the analysis were compared with that reported in the literature and it is concluded that the present formulation by incorporating the true variation of α with *GSI* significantly improves the existing solution(s) for *GSI* < 30.

ARTICLE HISTORY
Received 6 August 2019
Accepted 26 September 2019

KEYWORDS
Finite elements; Hoek and Brown yield criterion; limit analysis; nonlinear optimization; rocks

Introduction

The generalized Hoek–Brown (GHB) yield criterion (Hoek and Brown 1980, 1988, 1997; Hoek, Carranza-Torres, and Corkum 2002) is recommended as the most acceptable basis for checking the failure of intact and heavily jointed rock mass. For given input material strength parameters, this criterion, unlike the Mohr-Coulomb failure expression, provides a nonlinear relationship between the major and minor principal stresses. By using this failure criterion in combination with the limit analysis, a number of stability problems in rock mechanics have been solved (Yang, Li, and Yin 2004; Yang and Yin 2005; Merifield, Lyamin, and Sloan 2006; Saada, Maghous, and Garnier 2007; Li, Merifield, and Lyamin 2008; Chakraborty and Kumar 2015, 2016; Keshavaraz and Kumar 2017; Kumar and Mohapatra 2017, 2018). Yang, Li, and Yin (2004) evaluated the stability numbers for rock slopes by employing the log-spiral rupture mechanism while applying the kinematical approach of the limit analysis. Yang and Yin (2005) used the upper bound rigid blocks mechanism to obtain the ultimate bearing capacity of strip footings placed on rock mass. In this approach, the Mohr-Coulomb failure criterion was, however, used by defining its equivalent shear strength parameters in terms of the given yield parameters for the GHB yield expression. Merifield, Lyamin, and Sloan (2006) applied the numerical limit analysis, using both lower and upper bounds theorems, in combination with the nonlinear optimization procedure for solving plane strain problems using the GHB failure criterion. The yield surface was smoothed in the meridian plane in order to employ the nonlinear optimization technique. Saada, Maghous, and Garnier (2007) derived the closed form expression of the support function (power dissipation function) for the GHB under plane condition, and used it then to compute the ultimate bearing capacity of a strip footing resting on rock mass using the kinematical approach of the limit analysis. In this formulation, the collapse mechanism was assumed to comprise of a number of triangular rigid blocks emerging from the footing edge (singular point). Li, Merifield, and Lyamin (2008) produced stability charts for rock slopes by using the lower and upper bound finite element limit analysis method under plane strain condition; the Mohr-Coulomb failure criterion was, however, employed and its equivalent shear strength parameters, correlating with the GHB yield criterion, were used. Chakraborty and Kumar (2015) implemented the three-dimensional (3D) form of the generalized HB yield criterion for determining the bearing capacity of a circular footing over rock mass. In this formulation, the yield surface, which becomes a curvilinear pyramid in principal stress space, was smoothed in the meridian as well as the deviatoric planes. Kumar and Mohapatra (2017) used the *semidefinite programming* (SDP) technique to obtain the lower bound on the bearing capacity for a circular footing resting over rock mass by involving the GHB yield criterion. In this formulation, there was no need to smoothen the yield criterion. However, this approach is meant only for the case when the value of the exponent α, in the generalized HB criterion become equal to 0.5, so that one formulates the yield condition in terms of second-order conic constraints. Kumar and Mohapatra (2018) later proposed an iterative approximate procedure wherein the true value of α was accounted by reducing the material strength parameters. It is understood that an assumption of choosing $\alpha = 0.5$ affects the solution quite significantly for weak rocks when the value of *GSI* becomes smaller than about 30. For instance, in the case of a strip footing lying over weak rock mass, for *GSI*= 10, if the value of α is taken equal to 0.5, the value of N_σ is overestimated to an

CONTACT Manash Chakraborty manashchakra.civ@itbhu.ac.in Department of Civil Engineering, Indian Institute of Technology (BHU), Varanasi, India

extent of 200-250%. Therefore, there is a need to incorporate the true variation of α especially when the value of *GSI* becomes smaller than 30. This was the prime motivation for carrying out the present research work. In this study, the true variation of α with *GSI* has been incorporated in the analysis. The proposed formulation has been applied to evaluate the bearing capacity of a circular footing resting over homogenous and isotropic rock mass. Undoubtedly, the presence of rock mass provides an ideal location for laying the foundation. However, there is always a need to predict accurately the ultimate bearing capacity of foundations for structures which need to support heavy loads. The bearing capacity factor for a circular foundation on rock mass has been obtained for different values of material input parameters. The obtained results have been compared with the different solutions reported in the literature.

Generalized Hoek-Brown yield criterion and its smoothing

By performing a large number of triaxial tests at different stress levels on several rock samples, Hoek and Brown (Hoek and Brown 1980, 1988, 1997; Hoek, Carranza-Torres, and Corkum 2002) proposed the following relationship between major and minor principle stresses (σ_1, σ_3) to define the failure for intact and jointed rock mass:

$$\sigma_1 = \sigma_3 + \sqrt{-m\sigma_1\sigma_{ci} + s\sigma_{ci}^2} \tag{1}$$

where (i) σ_{ci} defines the uniaxial (unconfined) compressive strength of the intact rock mass sample, and (ii) m and s refer to dimensionless input material parameters. The original form of the Hoek-Brown yield criterion was later modified (Hoek and Brown 1997; Hoek, Carranza-Torres, and Corkum 2002) to take the following revised generalized form:

$$\sigma_1 = \sigma_3 + \left(-m_b\sigma_1\sigma_{ci}^{(1-\alpha)/\alpha} + s\sigma_{ci}^{1/\alpha}\right)^{\alpha} \tag{2}$$

Here the term m_b accounts for the broken rock mass and can be expressed as a function of m_i, geological strength index (*GSI*) and the disturbance factor D_f. The parameters m_b, s and α depends upon the material characteristics of the rock mass. The relationships among m_b, s and α with *GSI* and D_f are expressed by the following basic expressions:

$$m_b = m_i e^{(GSI-100)/\left(28-14D_f\right)} \tag{3a}$$

$$s = e^{(GSI-100)/\left(9-3D_f\right)} \tag{3b}$$

$$\alpha = \frac{1}{2} + \frac{1}{6}\left(e^{-GSI/15} - e^{-20/3}\right) \tag{3c}$$

The value of *GSI* varies from 10 to 100. For the value of *GSI* varying between 10 and 100, the exponent α, as per Eq. 3(c), varies between 0.59 and 0.50. For $GSI \geq 50$, the value of α becomes almost close to 0.50.

The GHB yield criterion given in Eq. (2) can be written in terms of three stress invariants ($\sigma_m, \dot{\sigma}$ and θ) as defined by Nayak and Zienkiewicz (1972). In terms of these stress invariants, the GHB criterion can be written in the following form for an axisymmetric problem:

$$f(\sigma) = (2\dot{\sigma}\cos\theta)^{(1/\alpha)} - m_b\sigma_{ci}^{(1-\alpha)/\alpha}\dot{\sigma}\left(\frac{\sin\theta}{\sqrt{3}} - \cos\theta\right) + m_b\sigma_{ci}^{(1-\alpha)/\alpha}\sigma_m - s\sigma_{ci}^{1/\alpha} = 0 \tag{4}$$

where

$$\text{(i)}\ \sigma_m = \frac{1}{3}(\sigma_r + \sigma_z + \sigma_\theta) \tag{5a}$$

$$\text{(ii)}\ \dot{\sigma} = \sqrt{0.5\left(s_r^2 + s_z^2 + s_\theta^2\right) + \tau_{rz}^2};\ s_i = \sigma_i - \sigma_m (i = r, z, \theta) \tag{5b}$$

$$\text{(iii)}\ -30^\circ \leq \theta = \sin^{-1}\left(-\frac{3\sqrt{3}}{2}\frac{J_3}{\dot{\sigma}^3}\right) \leq 30^\circ; J_3 = s_r s_z s_\theta - s_\theta\tau_{rz}^2 \tag{5c}$$

The GHB yield surface was plotted in principal stress space as well as in π-plane for two different values of *GSI*, namely, 10 and 70, with σ_{ci} = 100 MPa and m_i = 35. The shape of the yield surface is illustrated in Figure 1(a–c). The expansion of the yield surface can be clearly noted with an increase in the value of *GSI*. The yield surface exhibits discontinuities at (i) the corners of the hexagon in a π-plane, and (ii) the tip in a meridian plane, as shown in Figure 1(a). These stress discontinuities can be smoothed by employing (i) a quasi-hyperbolic approximation to deal with the presence of the tip discontinuity in a meridian plane, and (ii) trigonometric round off approach to smoothen the corners of the hexagon in π-plane (Sloan and Booker, 1986). Following the analysis of Merifield, Lyamin, and Sloan (2006), if the basic GHB yield criterion is expressed by replacing $\dot{\sigma}$ in Eq. (4) with $\ddot{\sigma}$, it will not then exhibit any sharp corner at the apex in the meridian plane:

where (i)$\ddot{\sigma} = \sqrt{\dot{\sigma}^2 + \varepsilon^2}$, (ii)$\varepsilon = \min(\delta, \mu\rho)$. Here, the value of (a) $\delta = 10^{-6}\sigma_{ci}$; $\mu = 10^{-1}$ and (b) ρ is evaluated from this equation: $-2\rho + \left(\rho m_b\sigma_{ci}^{(1-\alpha)/\alpha} + s\sigma_{ci}^{1/\alpha}\right)^{\alpha} = 0$.The stress discontinuities at the corners of the hexagon in a π-plane will, however, still exist. To smoothen these corners, a modified yield surface was proposed (Chakraborty and Kumar 2015). Upto a certain lode angle (denoted as transition angle, θ_T), the original HB yield criterion is followed and beyond $|\theta| \geq \theta_T$ the modified yield criterion is followed. The value of θ_T was chosen as 29.5°corresponding to the transition between the original and smoothed yield surface; note that the maximum possible absolute value of θ_T is 30°. The yield function, as defined in (Chakraborty and Kumar 2015), takes the following form:

For$|\theta| \geq \theta_T$, the smoothed expression for the yield surface:

$$f(\sigma) = m_b\sigma_{ci}^{(1-\alpha)/\alpha}\sigma_m - m_b\sigma_{ci}^{(1-\alpha)/\alpha}\ddot{\sigma}\left(A + B\sin 3\theta + C\sin^2 3\theta\right) - s\sigma_{ci}^2 = 0 \tag{6}$$

For$|\theta| < \theta_T$, the original HB expression:

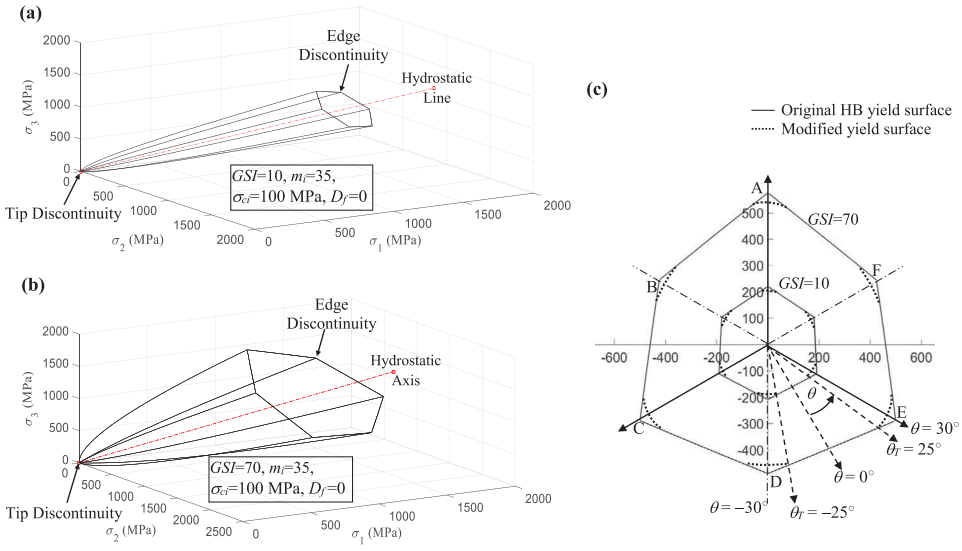

Figure 1. Representation of the HB yield surface for m_i = 35, σ_{ci} = 100 Mpa, D_f = 0 for GSI = 10 and 70 in (a, b) 3D principal stress space; and (c) π-plane with the smoothing of the vertices.

$$f(\sigma) = (2\ddot{\sigma}\cos\theta)^{1/\alpha} - m_b\sigma_{ci}^{(1-\alpha)/\alpha}\ddot{\sigma}\left(\frac{\sin\theta}{\sqrt{3}} - \cos\theta\right) + m_b\sigma_{ci}^{(1-\alpha)/\alpha}\sigma_m - s\sigma_{ci}^{1/\alpha} = 0 \quad (7)$$

In Eq. (6), there are three unknowns, namely, A, B and C; the expressions for which have been presented earlier by Chakraborty and Kumar (2015) and are not repeated herein. For a particular value of the hydrostatic stress (σ_m), the values of A, B and C become simply constant.

In the present article, the smoothed yield surface is generated by satisfying the following three criteria.

(i) At $|\theta| = \theta_T$, the value of $\ddot{\sigma}$ for the original and modified HB criteria becomes equal.
(ii) At $|\theta| = \theta_T$, the value of $\frac{\partial\ddot{\sigma}}{\partial\theta}$ for the original and modified HB criteria remains the same.
(iii) $\theta = \pm 30°$, the value of $\frac{\partial\ddot{\sigma}}{\partial\theta} = 0$.

Note that for the smoothed HB yield surface, irrespective of the value of θ, the values of $\ddot{\sigma}$ and $\frac{\partial\ddot{\sigma}}{\partial\theta}$ remain always continuous; the smoothed yield surface remains C_1 continuous.

Accordingly, for $|\theta| \geq \theta_T$, the following modified yield expression is formed which satisfies all the above three criteria:

$$f(\boldsymbol{\sigma}) = m_b\sigma_{ci}^{(1-\alpha)/\alpha} - m_b\sigma_{ci}^{\frac{1-\alpha}{\alpha}}\ddot{\sigma}(A + B\sin 3\theta) - s\sigma_{ci}^{1/\alpha} = 0 \quad (8)$$

Since the value of α varies between 0.50 and 0.59, the expression in Eq. (7) does not take a simple form and, hence, the parameters A and B cannot be evaluated directly simply by using the analytical approach, and need to be evaluated numerically.

Determining the values of A and B

If the value of θ evaluated from Eq. 5(c) exceeds θ_T, a modified yield surface expression is required. The values of A and B in the modified yield surface are evaluated by satisfying the first two conditions as mentioned in the previous section. At first, the value of $\ddot{\sigma}$ at $|\theta| = \theta_T$is evaluated from the original yield criterion Eq. (7) by using Newton–Raphson method. In the Newton–Raphson method, $\ddot{\sigma}$is updated in every stage by using the following equation:

$$\ddot{\sigma}_{modified} = \ddot{\sigma}_{previous} + f(\boldsymbol{\sigma})/f'(\boldsymbol{\sigma}) \quad (9)$$

The initial value of $\ddot{\sigma}$is taken to be equal to the $\ddot{\sigma}$value which is obtained by considering α to be 0.5 in Eq. (7). The evaluated value of $\ddot{\sigma}$is then reinserted in Eq. (8), which then generates the following equation:

$$(A + B\langle\psi\rangle\sin 3\theta_T) = \left(m_b\sigma_{ci}^{(1-\alpha)/\alpha}\sigma_m - s\sigma_{ci}^{1/\alpha}\right)/\left(m_b\sigma_{ci}^{(1-\alpha)/\alpha}\ddot{\sigma}\right) = k_3 \quad (10)$$

In this equation, $\langle\psi\rangle$represents the Macaulay brackets: (i)$\langle\psi\rangle$= 1, if θ is $\geq 0°$, and (ii)$\langle\psi\rangle = -1$, if θ is $< 0°$. Another equation is obtained by equating the values of $\frac{\partial\dot{\sigma}}{\partial\theta}$both for the original as well as the modified criterion.

$$\frac{\partial\dot{\sigma}}{\partial\theta_{\text{original}}} = \frac{\ddot{\sigma}}{\dot{\sigma}}\frac{k_1(2\ddot{\sigma}\langle\psi\rangle\sin\theta_T) + m_b\sigma_{ci}^{(1-\alpha)/\alpha}\ddot{\sigma}\left(\frac{\cos\theta_T}{\sqrt{3}} + \langle\psi\rangle\sin\theta_T\right)}{k_1(2\cos\theta_T) - m_b\sigma_{ci}^{(1-\alpha)/\alpha}\left(\frac{\langle\psi\rangle\sin\theta_T}{\sqrt{3}} - \cos\theta_T\right)} = \frac{\ddot{\sigma}}{\dot{\sigma}}k_2 \quad (11)$$

where $k_1 = \frac{1}{\alpha}(2\ddot{\sigma}\cos\theta_T)^{(1-\alpha)/\alpha}$

$$\frac{\partial\dot{\sigma}}{\partial\theta_{\text{modified}}} = -\frac{\ddot{\sigma}}{\dot{\sigma}}\frac{3B\ddot{\sigma}\cos 3\theta_T}{A + B\langle\psi\rangle\sin 3\theta_T} \quad (12)$$

Equating Eqs. (11) and (12):

$$\frac{\ddot{\sigma}}{\dot{\sigma}}k_2 = -\frac{\ddot{\sigma}}{\dot{\sigma}}\frac{3B\ddot{\sigma}\cos 3\theta_T}{A + B\langle\psi\rangle\sin 3\theta_T} \quad (13)$$

For a particular value of$\ddot{\sigma}$, the value of $(A + B\langle\psi\rangle\sin 3\theta_T)$ can be evaluated by using Eq. (10). The value of $(A + B\langle\psi\rangle\sin 3\theta_T)$ is

then inserted in Eq. (13) to find the value of B by the following expression:

$$B = -k_2 k_3/(3\dot{\sigma}\cos 3\theta_T) \tag{14}$$

Substituting the value of B in Eq. (10) provides the value of A as:

$$A = k_3 + (k_2 k_3 \langle\psi\rangle \tan 3\theta_T)/(3\ddot{\sigma}) \tag{15}$$

Unlike the previous formulation provided by Chakraborty and Kumar (2015), in the present analysis, the parameters A and B do not become constant at a particular mean stress value but rather these terms become a function of the deviatoric stress. During the analysis, whenever the absolute value of the lode angle exceeds 29.5°, the modified yield surface is employed by considering the parameters A and B as defined by Eqs. (14) and (15), respectively.

Lower bound finite element limit analysis

The lower bound limit analysis in conjunction with finite elements and nonlinear optimization has been used. The objective function is maximized subjected to a set of (i) linear and nonlinear, and (ii) equality and inequality constraints. The linear equality constraints arise from (i) element equilibrium equations, (ii) stress discontinuity equations associated with the adjacent boundaries between the elements, (iii) stress boundary conditions. The nonlinear inequality constraints emerge, on the other hand, from the usage of the GHB yield criterion. The optimization problem is solved by using the interior point method. The procedure for solving a problem with the usage of the Mohr-Coulomb criterion has been elaborated in Chakraborty and Kumar (2014). This procedure was accordingly changed to account for the GHB yield criterion for the true value of α. The step-by-step procedure is mentioned in Appendix 1. While performing the nonlinear optimization it is

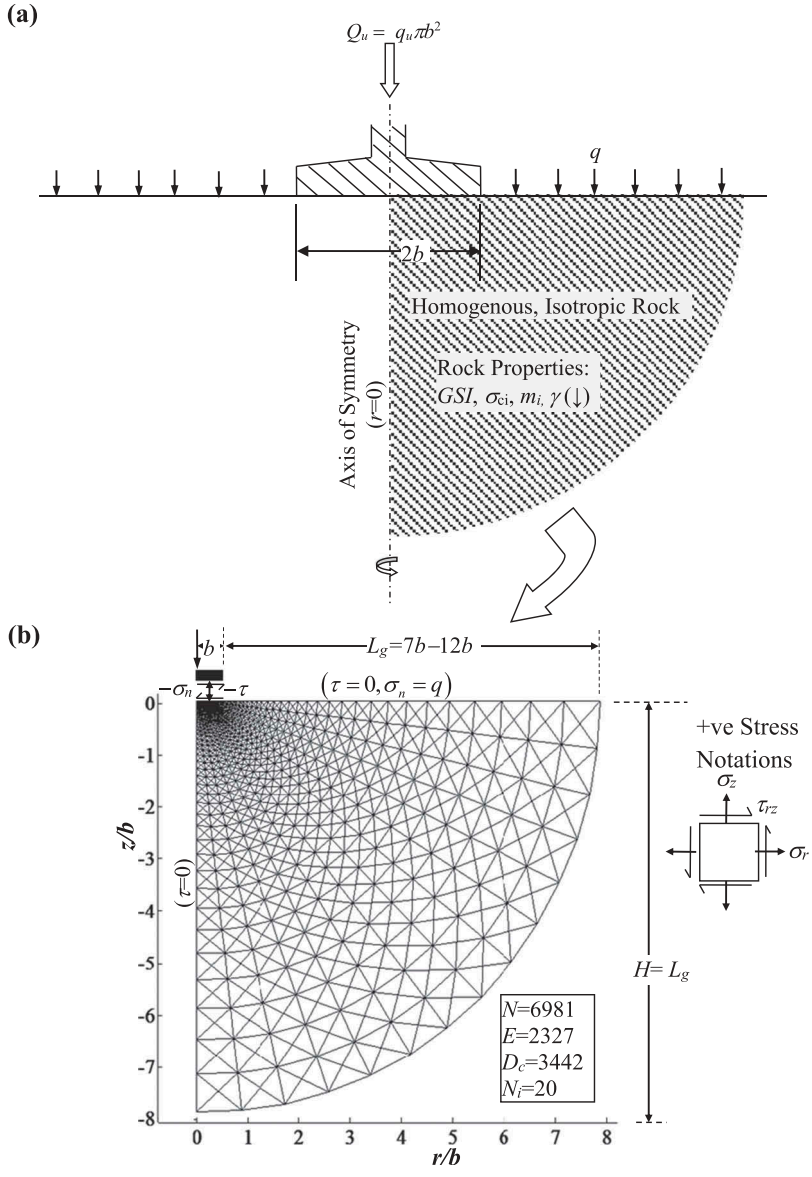

Figure 2. (a) Chosen domain and mesh for a circular footing for *GSI*= 90 and m_i= 40.

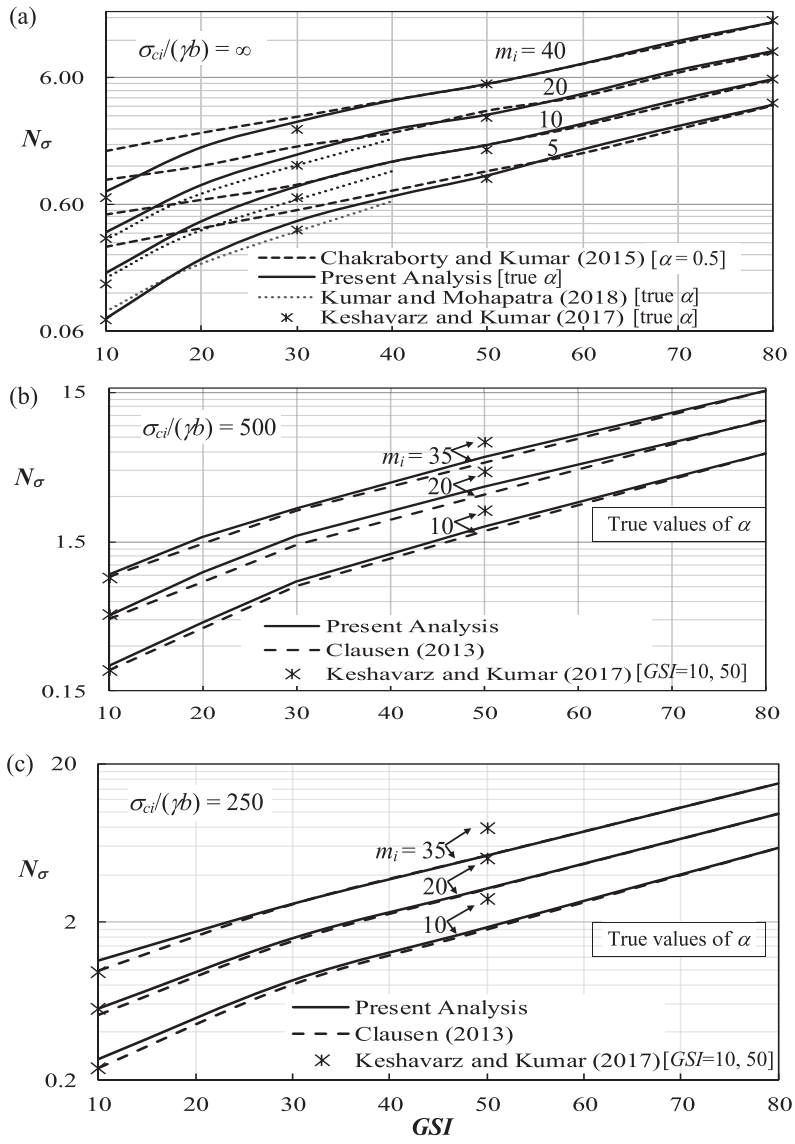

Figure 3. The variation of N_σ with *GSI* for different values of m_i with (a) $\sigma_{ci}/(\gamma b) = \infty$; (b) $\sigma_{ci}/(\gamma b) = 500$; and (c) $\sigma_{ci}/(\gamma b) = 250$.

required to obtain the gradient and Hessian matrices of the yield function. The gradient and the Hessian matrices of the original, as well as the modified HB yield function, are presented in Appendix 2. Starting from the initial values, the unknown stress vector is updated in each iteration based on the gradient and the Hessian matrices till the convergence is attained.

Implementation: bearing capacity of circular footing over rock mass

Definition of the problem

To examine the efficacy of the proposed formulation, the ultimate bearing capacity of a rough circular footing is evaluated. The radius of the footing is b and is subjected to vertical downward load (Q) without having any eccentricity. The footing is placed over horizontal rock surface which is loaded with surcharge pressure q. The rock mass is assumed to be perfectly plastic and it obeys the associated flow rule; its unit weight is defined by γ.

Domain, boundary conditions and FE mesh

The chosen domain and the associated boundary conditions are illustrated in Figure 2(a,b). The horizontal and vertical boundaries of the domain are chosen such that the failure zone is contained well within the specified domain and any further extension of the domain does not affect the magnitude of the collapse load. Three-noded linear triangular elements are used to model the stress field. The sizes of the elements were gradually reduced towards the footing edge. A typical chosen mesh is shown in Figure 2(b). The rock-footing interface is modelled to be perfectly rough. As a result, the yield strength of the footing-rock interface is dictated by the yield criterion for the rock mass itself.

The bearing capacity factor n_σ

The ultimate bearing capacity (q_u) is computed by using the expression:

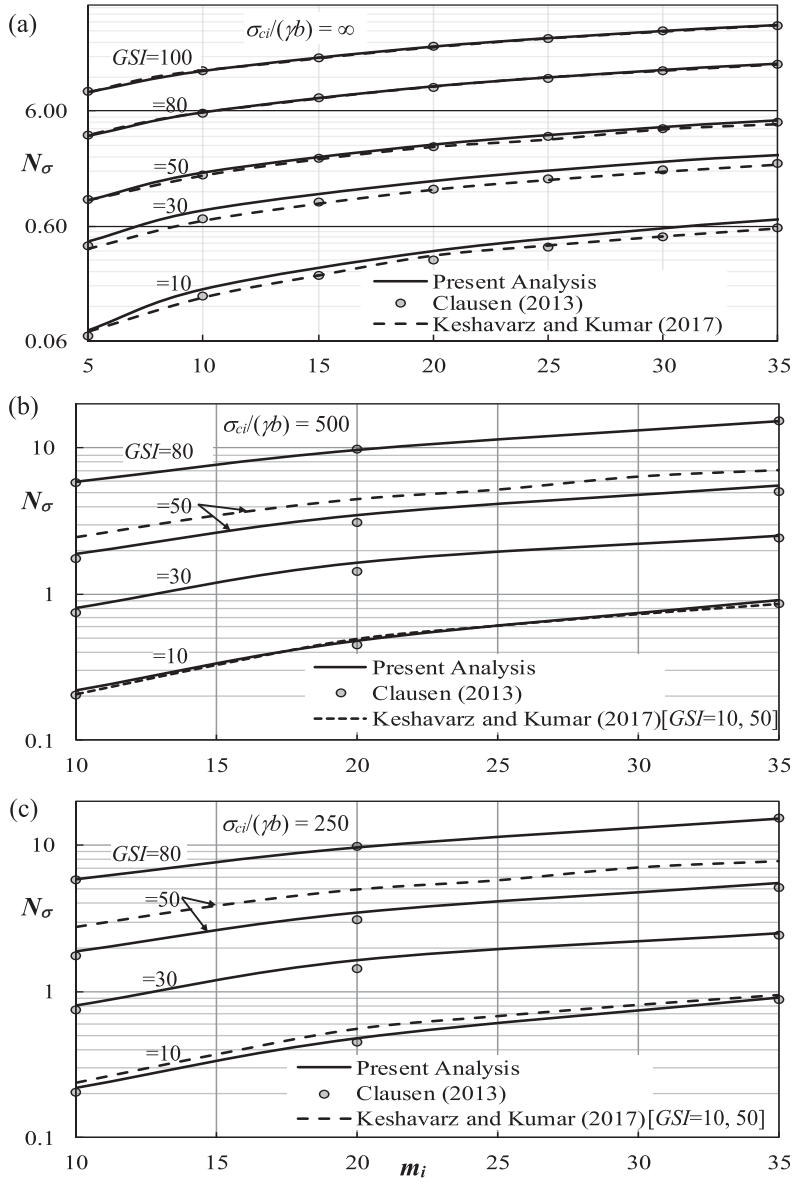

Figure 4. The variation of N_σ with m_i for different values of *GSI* with (a) $\sigma_{ci}/(\gamma b) = \infty$; (b) $\sigma_{ci}/(\gamma b) = 500$; and (c) $\sigma_{ci}/(\gamma b) = 250$.

$$q_u = \frac{Q_u}{(\pi b^2)} = \sigma_{ci} N_\sigma \tag{16}$$

Here N_σ refers to the bearing capacity factor which becomes a function of σ_{ci}, *GSI*, m_i and q/σ_{ci}.

Results and comparisons

The results are presented in the form of the bearing capacity factor N_σ.

Figure 3(a) presents the bearing-capacity factor, N_σ, for different combinations of *GSI* and m_i; in this case, it is assumed that the rock mass is weightless and no surcharge is added on ground surface. It can be noted that the magnitude of N_σ increases continuously with an increase in the values of both *GSI* and m_i. The increment becomes more significant for lower values of *GSI* and m_i. This figure also provides the comparison of the present results with that reported earlier by the authors for a constant value of $\alpha = 0.5$. Note that for the values of *GSI*< 40, the present analysis provides lower values of N_σ than that reported earlier by the authors by assuming$\alpha = 0.5$. Note that the difference between the two solutions keeps on increasing with a decrease in the value of *GSI*. The present solutions were further compared with that reported by (i) Keshavaraz and Kumar (2017) on the basis of the method of stress characteristics and (ii) Kumar and Mohapatra (2018) on the basis of the lower bound finite elements limit analysis in combination with semidefinite programming (SDP). In the work of Kumar and Mohapatra (2018), the variation of α with *GSI* was taken indirectly by changing the material strength parameters. The solutions from the three different methods (the current NLP procedure, the method of stress characteristics and the SDP technique) seem to compare well with each other.

Figure 3(b,c) present the variation of the bearing capacity factor N_σ with *GSI* and m_i considering the unit weight (γ) of the rock mass. The solutions are presented for two different values of $\sigma_{ci}/(\gamma b)$, namely, 250 and 500.The value of N_σ

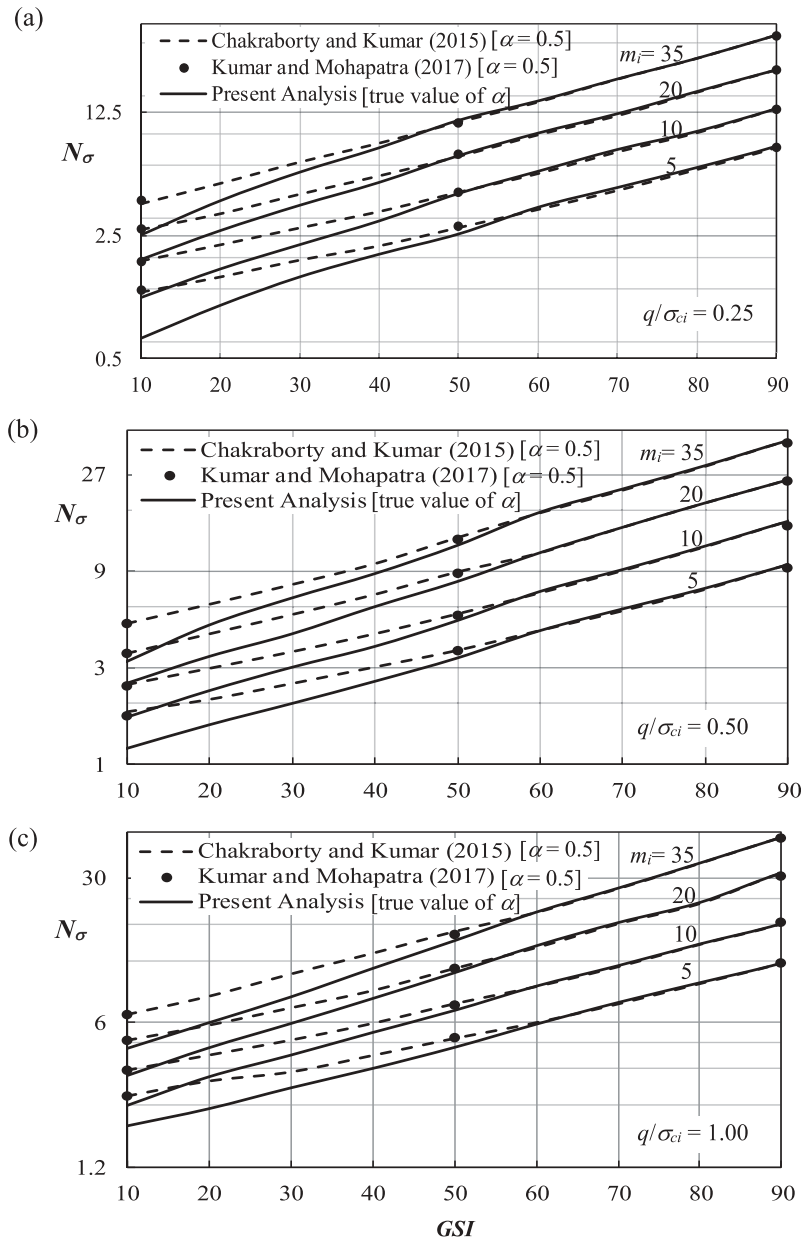

Figure 5. The variation of N_σ with *GSI* for a weightless rock media for different values of m_i with (a) $q/\sigma_{ci} = 0.25$; (b) $q/\sigma_{ci} = 0.5$; and (c) $q/\sigma_{ci} = 1.0$.

increases continuously with an increase in γ, that is, with a decrease in the value of $\sigma_{ci}/(\gamma b)$. However, this increment of N_σ with an increase in γ is found to be more significant for the value of *GSI* smaller than 50. For *GSI* > 50, the values of N_σ for weightless and ponderable rock mass are found to be more or less the same. The results from the present analysis were also compared with the displacement-based elastoplastic finite element solutions obtained by Clausen (2013) and the stress characteristics' solutions given by Keshavaraz and Kumar (2017) for true values of α. Keshavaraz and Kumar (2017) provided the solutions for only two values *GSI*, namely, 10 and 50. Note that the present solutions match quite well with the finite element results of Clausen (2013); however, the the values of N_σ from the present analysis are lower than the solutions provided by Keshavaraz and Kumar (2017) for *GSI* = 50. It needs to be mentioned that the method of characteristic solution is based on the assumption of the value of the circumferential stress (σ_θ). On the other hand, neither the present analysis nor the SDP procedure requires this assumption associated with σ_θ.

Figure 4 shows the variation of N_σ with m_i corresponding to different values of *GSI*. The figure also depicts a comparison between the present solution and that provided by Clausen (2013) and Keshavaraz and Kumar (2017). For a weightless rock mass, all the three solutions match well with each other; however, as the unit weight of the rock is incorporated in the analysis, the deviation of the solution reported by Keshavaraz and Kumar (2017) become quite noteworthy with respect to the other two. The reason of this deviation can be attributed to the fact that σ_θ was considered equal to the value of σ_3 in the work of Keshavaraz and Kumar (2017); no such assumption regarding σ_θ is required in the present analysis.

Figure 5 depicts the effect of surcharge (q) on the values of N_σ for different combinations of *GSI* and m_i corresponding to $\sigma_{ci}/(\gamma b) = 250$. Three different values of q/σ_{ci}, namely, 0.25, 0.50 and 1 were used. It can be seen that with an increase in q/σ_{ci}, there is a considerable increment in N_σ. In this figure, the results were compared with the lower bound solutions provided by Chakraborty and Kumar (2015) and Kumar and Mohapatra (2017) but with an assumption of $\alpha = 0.5$. It can be noted that for the value of GSI < 50, the present analysis provides relatively lower values of N_σ than that computed with an assumption of $\alpha = 0.5$. Note that the difference between the existing solutions and the present one becomes quite substantial for the value of *GSI* between 10 and 30.

Conclusions

On the basis of the axisymmetric lower bound finite elements limit analysis in combination with nonlinear optimization, a formulation has been presented to incorporate the true variation of the exponent factor α with *GSI* while using the generalized Hoek and Brown yield criterion. By using the proposed formulation, the bearing capacity factor for a rough circular footing, placed over rock mass, has been determined for different values of *GSI*, m_i, q/σ_{ci} and $\sigma_{ci}/(\gamma b)$. No assumption is involved associated with either the exponent α in the yield expression or the circumferential stress σ_θ. Especially for values of *GSI* smaller than 30, the proposed formulation significantly improves the existing solutions which are generally meant for $\alpha = 0.5$. The formulation can be employed to determine the solution of any axisymmetric stability problem in rock mechanics on the basis of the generalized Hoek and Brown yield criterion.

Disclosure statement

No potential conflict of interest was reported by the authors.

References

Chakraborty, M., and J. Kumar. 2014. "Lower Bound Axisymmetric Formulation for Geomechanics Problems Using Nonlinear Optimization." *International Journal Of Geomechanics* 15 (5): 06014024. doi: 10.1061/(ASCE)GM.1943-5622.0000454.

Chakraborty, M., and J. Kumar. 2015. "Bearing Capacity Of Circular Footings over Rock Mass by Using Axisymmetric Quasi Lower Bound Finite Element Limit Analysis." *Computers and Geotechnics* 70: 138–149. doi: 10.1016/j.compgeo.2015.07.015.

Chakraborty, M., and J. Kumar. 2016. "Reply to Discussion on "bearing Capacity of Circular Footings over Rock Mass by Using Axisymmetric Quasi Lower Bound Finite Element Limit Analysis." *Computers and Geotechnics* 73: 235–237. doi:10.1016/j.compgeo.2015.12.004.

Clausen, J. 2013. "Bearing Capacity of Circular Footings on a Hoek–Brown Material." *International Journal of Rock Mechanics and Mining Sciences* 57: 34–41. doi:10.1016/j.ijrmms.2012.08.004.

Hoek, E., C. Carranza-Torres, and B. Corkum 2002. "Hoek–Brown Failure Criterion-2002 Edition." *Proceedings of North American Rock Mechanics Society*, Meeting in Toronto.

Hoek, E., and E. T. Brown. 1980. "Empirical Strength Criterion for Rock Masses." *Journal of Geotechnical Engineering Division* 106 (9): 1013–1035.

Hoek, E., and E. T. Brown 1988. "The Hoek–Brown Failure Criterion – A 1988 Update. In: Rock Engineering for Underground Excavations." *Proceedings of 15th Canadian Rock Mechanics Symposium*, University of Toronto; 31–38.

Hoek, E., and E. T. Brown. 1997. "Practical Estimates of Rock Mass Strength." *International Journal of Rock Mechanics and Mining Sciences* 34 (8): 1165–1186. doi:10.1016/S1365-1609(97)80069-X.

Keshavaraz, A., and J. Kumar. 2017. "Bearing Capacity of Foundations on Rock Mass Using the Method of Stress Characteristics." *International Journal of Numerical and Analytical Methods in Geomechanics* 42 (3): 542–557. doi:10.1002/nag.2754.

Kumar, J., and D. Mohapatra. 2017. "Lower-bound Finite Elements Limit Analysis for Hoek-brown Materials Using Semidefinite Programming." *Journal Of Engineering Mechanics* 143 (9): 04017077. doi: 10.1061/(ASCE)EM.1943-7889.0001296.

Kumar, J., and D. Mohapatra. 2018. "Closure to Lower-bound Finite Elements Limit Analysis for Hoek-brown Materials Using Semidefinite Programming." *Journal Of Engineering Mechanics* 144 (7): 07018002. doi: 10.1061/(ASCE)EM.1943-7889.0001486.

Li, A. J., R. S. Merifield, and A. V. Lyamin. 2008. "Stability Charts for Rock Slopes Based on the Hoek–Brown Failure Criterion." *International Journal of Rock Mechanics and Mining Sciences* 45: 689–700. doi:10.1016/j.ijrmms.2007.08.010.

Merifield, R. S., A. V. Lyamin, and S. W. Sloan. 2006. "Limit Analysis Solutions for the Bearing Capacity of Rock Masses Using the Generalised Hoek–Brown Yield Criterion." *International Journal of Rock Mechanics and Mining Sciences* 43: 920–937. doi:10.1016/j.ijrmms.2006.02.001.

Nayak, G. C., and O. C. Zienkiewicz. 1972. "Convenient Form of Stress Invariants for Plasticity." *Journal of Structure Division* 98: 949–954.

Saada, Z., S. Maghous, and D. Garnier. 2007. "Bearing Capacity of Shallow Foundations on Rocks Obeying a Modified Hoek–Brown Failure Criterion." *Computers and Geotechnics* 35: 144–154. doi:10.1016/j.compgeo.2007.06.003.

Sloan, S. W., and J. R. Booker. 1986. "Removal of Singularities in Tresca and Mohr-Coulomb Yield Functions." *Communication and Applied Numerical Methods* 2: 173–179. doi:10.1002/cnm.1630020208.

Yang, X. L., and J. H. Yin. 2005. "Upper Bound Solution for Ultimate Bearing Capacity with a Modified Hoek–Brown Failure Criterion." *International Journal of Rock Mechanics and Mining Sciences* 42: 550–560. doi:10.1016/j.ijrmms.2005.03.002.

Yang, X. L., L. Li, and J. H. Yin. 2004. "Stability Analysis of Rock Slopes with a Modified Hoek–Brown Failure Criterion." *International Journal of Numerical and Analytical Methods in Geomechanics* 28 (2): 181–190. doi:10.1002/nag.330.

Appendix 1

The optimization form of the circular footing problem (by adding the log-barrier function) is as following:

$$\text{Maximize: } w = \boldsymbol{b}^T\boldsymbol{\sigma} + \mu^k \sum_{j=1}^{(N+4t)} \log s_j$$
$$\text{Subjected to: } \boldsymbol{A_{eq}\sigma} = B_{eq} \text{ and } \boldsymbol{g}(\sigma) + \boldsymbol{s} = 0$$

where (i) $\boldsymbol{b}$ is a n-dimensional vector containing coefficient terms of the objective function; (ii) $\boldsymbol{A_{eq}}$ and $\boldsymbol{B_{eq}}$ are the coefficient matrix and the right-hand side vector of equality constraints; (iii) μ^k is a barrier parameter; (iv) $\boldsymbol{s}$ is the slack variable and (v) $g(\boldsymbol{\sigma})$ denotes the inequality constraints emerge from the GHB yield criterion and the soil-footing roughness conditions. Here, n, l, k and t define the numbers of unknown stress variables, equality constraints, iterations and soil-foundation boundary edges, respectively.

The Lagrangian polynomial function for this optimization problem is:

$$L(\boldsymbol{\sigma}, \boldsymbol{s}, \boldsymbol{\lambda}, \boldsymbol{v}) = \boldsymbol{b}^T\boldsymbol{\sigma} + \mu^k \sum_{j=1}^{(N+4t)} \log s_j - \boldsymbol{\lambda}^T(g(\boldsymbol{\sigma}) + \boldsymbol{s}) - \boldsymbol{v}^T(\boldsymbol{B_{eq}} - \boldsymbol{A_{eq}\sigma})$$

where $\boldsymbol{\lambda}$ and $\boldsymbol{v}$ are the Lagrangian multiplier corresponding to inequality and equality constraints, respectively. KKT optimality conditions are employed.

The algorithm for solving this nonlinear optimization is mentioned step by step in the following:

Step-1: Initialization: $\boldsymbol{\sigma}^0 = e, \boldsymbol{s}^0 = e, \boldsymbol{\lambda}^0 = e, \boldsymbol{v}^0 = 0$

Step-2: Assigning $\boldsymbol{\mu^k}$: $\boldsymbol{\mu}^k = 0.2(\boldsymbol{s}^0)^T\boldsymbol{\lambda}^0/(N+4t)$

Step-3: Calculating Residuals:

$$\begin{aligned} \boldsymbol{r}_{1_{(n,1)}} &= \nabla g(\boldsymbol{\sigma})\boldsymbol{\lambda} - \boldsymbol{A_{eq}}^T\boldsymbol{v} - \boldsymbol{b} \\ \boldsymbol{r}_{2_{(N+4t,1)}} &= \boldsymbol{S\lambda} - \mu^k\boldsymbol{e} \\ \boldsymbol{r}_{3_{(N+4t,1)}} &= g(\boldsymbol{\sigma}) + \boldsymbol{s} \\ \boldsymbol{r}_{4_{(l,1)}} &= \boldsymbol{B_{eq}} - \boldsymbol{A_{eq}\sigma} \end{aligned}$$

Step-4:Determining $\Delta\boldsymbol{v}$ from the following equation:

$$(\boldsymbol{A_{eq}W}^{-1}\boldsymbol{A}_{eq}^T)_{(l\times l)}\Delta\boldsymbol{v}_{(l\times 1)} = (\boldsymbol{r}_4 + \boldsymbol{A_{eq}W}^{-1}\boldsymbol{q})_{(l\times 1)}$$

where $\boldsymbol{W} = (\boldsymbol{H} + \nabla g\boldsymbol{S}^{-1}\boldsymbol{\Lambda}\nabla g^T)$ and $\boldsymbol{q} = \boldsymbol{r}_1 + \nabla g\boldsymbol{S}^{-1}(\boldsymbol{\Lambda r}_3 - \mathbf{r}_2)$

Step-5: Computing $\Delta\boldsymbol{\sigma}$, $\Delta\boldsymbol{s}$, $\Delta\boldsymbol{\lambda}$

$$\Delta\boldsymbol{\sigma}_{(n\times 1)} = \boldsymbol{W}^{-1}_{(n\times n)}(\boldsymbol{A}^T_{eq(n\times l)}\Delta\boldsymbol{v}_{(l\times 1)} - \boldsymbol{q}_{(n\times 1)})$$

$$\Delta\boldsymbol{s}_{(N+4t,1)} = -(\mathbf{r}_{3(N+4t,1)} + \nabla g^T_{(N+4t,n)}\Delta\boldsymbol{\sigma}_{(n,1)})$$

$$\Delta\lambda_{(N+4t,1)} = -S^{-1}_{(N+4t,N+4t)}(r_{2(N+4t,1)} + \Lambda_{(N+4t,N+4t)}\Delta s_{(N+4t,1)})$$

Step-6: Evaluating Step-length: $\eta_D = \zeta\eta_D{}^{\max}$, $\eta_P = \zeta\eta_P{}^{\max}$

where, (i) ζ is adopted to be 0.90 and (ii)$\eta_D{}^{\max} = \min_{\Delta s_i<0}\left(-\frac{s_i{}^{k-1}}{s_i}\right)$;$\eta_P{}^{\max} = \min_{\Delta\lambda_i<0}\left(-\frac{\lambda_i{}^{k-1}}{\lambda_i}\right)$

Step-7: Updating Unknown Variables

$$\boldsymbol{\sigma}^k_{(n\times 1)} = \boldsymbol{\sigma}^{k-1}_{(n\times 1)} + \eta_D\Delta\boldsymbol{\sigma}_{(n\times 1)}$$

$$\boldsymbol{s}^k_{(N+4t,1)} = \boldsymbol{s}^{k-1}_{(N+4t,1)} + \eta_D\Delta\boldsymbol{s}_{(N+4t,1)}$$

$$\boldsymbol{\lambda}^k_{(N+4t,1)} = \boldsymbol{\lambda}^{k-1}_{(N+4t,1)} + \eta_P\Delta\boldsymbol{\lambda}_{(N+4t,1)}$$

$$\boldsymbol{v}^k_{(l\times 1)} = \boldsymbol{v}^{k-1}_{(l\times 1)} + \eta_P\Delta\boldsymbol{v}_{(l\times 1)}$$

Step-8: Convergence Check

Steps 1 to 7 are repeated until the convergence $(abs((\boldsymbol{b}^T\boldsymbol{\sigma})^k - (\boldsymbol{b}^T\boldsymbol{\sigma})^{k-1}) < 10^{-5})$ is attained.

Step-9: Updating $\boldsymbol{\mu^k}$: Until convergence, μ^k is updated in the next iteration as follows:

$$\mu^k = 0.2(s^k)^T\boldsymbol{\lambda}^k/(N+4t)$$

Appendix 2

Yield function form

$$f(\boldsymbol{\sigma}) = (2\ddot{\sigma}\cos\theta)^{\frac{1}{\alpha}} - m_b\sigma_{ci}^{\frac{1-\alpha}{\alpha}}\ddot{\sigma}\left(\frac{\sin\theta}{\sqrt{3}} - \cos\theta\right) + m_b\sigma_{ci}^{\frac{1-\alpha}{\alpha}}\sigma_m - s\sigma_{ci}^{\frac{1}{\alpha}} = 0 \text{for} |\theta| < \theta_T$$

$$= m_b\sigma_{ci}^{(1-\alpha)/\alpha} - m_b\sigma_{ci}^{\frac{1-\alpha}{\alpha}}\ddot{\sigma}(A + B\sin 3\theta) - s\sigma_{ci}^{1/\alpha} = 0 \text{for} |\theta| \geq \theta_T$$

Gradient calculation

$$\nabla f = \frac{\partial f}{\partial \boldsymbol{\sigma}} = C_1\frac{\partial \sigma_m}{\partial \boldsymbol{\sigma}} + C_2\frac{\partial \dot{\sigma}}{\partial \boldsymbol{\sigma}} + C_3\frac{\partial J_3}{\partial \boldsymbol{\sigma}}$$

$$\frac{\partial \sigma_m}{\partial \boldsymbol{\sigma}} = \frac{1}{3}\begin{Bmatrix} 1 \\ 1 \\ 1 \\ 1 \end{Bmatrix};\ \frac{\partial \dot{\sigma}}{\partial \boldsymbol{\sigma}} = \frac{1}{2\dot{\sigma}}\begin{Bmatrix} s_r \\ s_z \\ 2\tau_{rz} \\ s_\theta \end{Bmatrix};\ \frac{\partial J_3}{\partial \boldsymbol{\sigma}} = \begin{Bmatrix} s_r s_\theta + \frac{\dot{\sigma}^2}{3} \\ s_z s_\theta + \frac{\dot{\sigma}^2}{3} \\ -2s_\theta\tau_{rz} \\ s_z s_r - \tau_{rz}^2 + \frac{\dot{\sigma}^2}{3} \end{Bmatrix}$$

(i) for $|\theta| < \theta_T$,

$$C_1 = \frac{\partial f}{\partial \sigma_m} = m_b\sigma_{ci}^{(1-\alpha)/\alpha}$$

$$C_2 = \frac{\partial f}{\partial \dot{\sigma}} - \frac{\tan 3\theta}{\dot{\sigma}}\frac{\partial f}{\partial \theta} = \frac{\dot{\sigma}}{\ddot{\sigma}}k_4 + \frac{\ddot{\sigma}}{\dot{\sigma}}k_5\tan 3\theta$$

$$C_3 = -\frac{\sqrt{3}}{2\cos 3\theta\,\dot{\sigma}^3}\frac{\partial f}{\partial \theta} = \frac{\ddot{\sigma}\sqrt{3}k_5}{2\cos 3\theta\dot{\sigma}^3}$$

where, $k_4 = -m_b\sigma_{ci}^{(1-\alpha)/\alpha}\left(\frac{\sin\theta}{\sqrt{3}} - \cos\theta\right) + \frac{1}{\alpha}(2\cos\theta)^{(1/\alpha)}\ddot{\sigma}^{(1-\alpha)/\alpha}$

$$k_5 = m_b\sigma_{ci}^{(1-\alpha)/\alpha}\left(\frac{\cos\theta}{\sqrt{3}} + \sin\theta\right) + \frac{1}{\alpha}(2\ddot{\sigma}\cos\theta)^{(1-\alpha)/\alpha}(2\sin\theta)$$

(ii) for $|\theta| \geq \theta_T$,

$$C_1 = \frac{\partial f}{\partial \sigma_m} = m_b\sigma_{ci}^{(1-\alpha)/\alpha}\left(\frac{k_2\sin 3\theta}{3\cos 3\theta_T} - \frac{1}{3}k_2\tan 3\theta_T\right)$$

$$C_2 = \frac{\partial f}{\partial \dot{\sigma}} - \frac{\tan 3}{\dot{\sigma}}\frac{\partial f}{\partial \theta}$$

$$= -\frac{\dot{\sigma}}{\ddot{\sigma}}m_b\sigma_{ci}^{\frac{1-\alpha}{\alpha}}(A + B\sin 3\theta) - m_b\sigma_{ci}^{\frac{1-\alpha}{\alpha}}\ddot{\sigma}\left(\frac{\partial A}{\partial \dot{\sigma}} + \frac{\partial B}{\partial \dot{\sigma}}\sin 3\theta - \frac{3B\sin 3\theta}{\dot{\sigma}}\right)$$

$$C_3 = -\frac{\sqrt{3}}{2\cos 3\theta\,\dot{\sigma}^3}\frac{\partial f}{\partial \theta} = -\frac{3B\sqrt{3}}{2\dot{\sigma}^3}m_b\sigma_{ci}^{\frac{1-\alpha}{\alpha}}\ddot{\sigma}$$

where

$$\frac{\partial A}{\partial \dot{\sigma}} = \frac{\partial k_3}{\partial \dot{\sigma}} + \frac{\tan 3\theta_T}{3}\left(k_2\frac{\partial k_3}{\partial \dot{\sigma}} + k_3\frac{\partial k_2}{\partial \dot{\sigma}}\right) = R_3 + \frac{\tan 3\theta_T}{3}(k_2R_3 + k_3R_2)$$

$$\frac{\partial B}{\partial \dot{\sigma}} = -\frac{1}{3\cos 3\theta_T}\left(k_2\frac{\partial k_3}{\partial \dot{\sigma}} + k_3\frac{\partial k_2}{\partial \dot{\sigma}}\right) = -\frac{1}{3\cos 3\theta_T}(k_2R_3 + k_3R_2)$$

$$R_1 = \frac{\partial k_1}{\partial \dot{\sigma}} = \frac{\dot{\sigma}}{\ddot{\sigma}}\frac{(1-\alpha)}{\alpha}(2\cos\theta_T)(2\ddot{\sigma}\cos\theta_T)^{(1-2\alpha)/\alpha}$$

$$R_2 = \frac{\partial k_2}{\partial \dot{\sigma}} = \frac{1}{P_2}\left(P_1\frac{\dot{\sigma}}{\ddot{\sigma}^2} + (2R_1\ddot{\sigma}\langle\psi\rangle\sin\theta_T)\right) - \frac{2P_1R_1\cos\theta_T}{P_2^2}$$

$$R_3 = \frac{\partial k_3}{\partial \dot{\sigma}} = \frac{s\sigma_{ci}^2 - m_b\sigma_{ci}^{(1-\alpha)/\alpha}\sigma_m}{m_b\sigma_{ci}^{(1-\alpha)/\alpha}}\left(\frac{\dot{\sigma}}{\ddot{\sigma}^3}\right)$$

$$P_1 = k_1(2\ddot{\sigma}\langle\psi\rangle\sin\theta_T) + m_b\sigma_{ci}^{(1-\alpha)/\alpha}\ddot{\sigma}\left(\frac{\cos\theta_T}{\sqrt{3}} + \langle\psi\rangle\sin\theta_T\right)$$

$$P_2 = k_1(2\cos\theta_T) - m_b\sigma_{ci}^{(1-\alpha)/\alpha}\left(\frac{\langle\psi\rangle\sin\theta_T}{\sqrt{3}} - \cos\theta_T\right)$$

Hessian calculation

$$\nabla^2 f = \frac{\partial C_2}{\partial \boldsymbol{\sigma}}\frac{\partial \dot{\sigma}}{\partial \boldsymbol{\sigma}} + C_2\frac{\partial^2 \dot{\sigma}}{\partial \boldsymbol{\sigma}^2} + \frac{\partial C_3}{\partial \boldsymbol{\sigma}}\frac{\partial J_3}{\partial \boldsymbol{\sigma}} + C_3\frac{\partial^2 J_3}{\partial \boldsymbol{\sigma}^2}$$

$$\frac{\partial C_2}{\partial \boldsymbol{\sigma}} = \frac{\partial C_2}{\partial \dot{\sigma}}\frac{\partial \dot{\sigma}}{\partial \boldsymbol{\sigma}} + \frac{\partial C_2}{\partial \theta}\frac{\partial \theta}{\partial \boldsymbol{\sigma}}$$

$$\frac{\partial C_3}{\partial \boldsymbol{\sigma}} = \frac{\partial C_3}{\partial \dot{\sigma}}\frac{\partial \dot{\sigma}}{\partial \boldsymbol{\sigma}} + \frac{\partial C_3}{\partial \theta}\frac{\partial \theta}{\partial \boldsymbol{\sigma}}$$

$$\frac{\partial C_2}{\partial \dot{\sigma}} = \frac{(1-\alpha)}{\alpha^2}\ddot{\sigma}^{\frac{1-2\alpha}{\alpha}}(2\cos\theta)^{\left(\frac{1}{\alpha}\right)}[1+\tan 3\theta\tan\theta] + k_5\tan 3\theta\left(\frac{1}{\ddot{\sigma}} - \frac{\ddot{\sigma}}{\dot{\sigma}^2}\right)$$

$$\left[\frac{(2\cos\theta)^{\left(\frac{1}{\alpha}\right)}\ddot{\sigma}^{\frac{1-\alpha}{\alpha}}}{\alpha} - m_b\sigma_{ci}^{(1-\alpha)/\alpha}\left(\frac{\sin\theta}{\sqrt{3}} - \cos\theta\right)\left(\frac{1}{\ddot{\sigma}} - \frac{\dot{\sigma}^2}{\ddot{\sigma}^3}\right)\right] = M_1$$

$$\frac{\partial C_3}{\partial \dot{\sigma}} = \frac{\ddot{\sigma}\sqrt{3}}{\left(2\cos 3\theta\dot{\sigma}^3\right)}\left(\frac{(1-\alpha)}{\alpha^2}\frac{\dot{\sigma}}{\ddot{\sigma}}(2\sin 2\theta)(2\ddot{\sigma}\cos\theta)^{\frac{1-2\alpha}{\alpha}} + k_5\left(\frac{\dot{\sigma}}{\ddot{\sigma}^2} - \frac{3}{\dot{\sigma}}\right)\right) = M_2$$

$$\frac{\partial C_3}{\partial \theta} = \frac{\ddot{\sigma}\,3\sqrt{3}k_5\tan 3\theta}{\left(2\cos 3\theta\dot{\sigma}^3\right)} + \frac{\ddot{\sigma}\sqrt{3}}{\left(2\cos 3\theta\dot{\sigma}^3\right)}\begin{pmatrix} m_b\sigma_{ci}^{(1-\alpha)/\alpha}\left(\cos\theta - \frac{\sin\theta}{\sqrt{3}}\right) + \frac{(2\cos\theta)^{1/\alpha}\ddot{\sigma}^{(1-\alpha)/\alpha}}{\alpha} \\ -\frac{(1-\alpha)}{\alpha^2}(4\ddot{\sigma}\sin^2\theta)(2\ddot{\sigma}\cos\theta)^{(1-2\alpha)/\alpha} \end{pmatrix} = M_3$$

$$\frac{\partial C_2}{\partial \theta} = \frac{\dot{\sigma}}{\ddot{\sigma}}\left(\frac{-2\sin\theta}{\alpha^2}(2\ddot{\sigma}\cos\theta)^{(1-\alpha)/\alpha} - m_b\sigma_{ci}^{(1-\alpha)/\alpha}\left(\sin\theta + \frac{\cos\theta}{\sqrt{3}}\right)\right) + \frac{3\ddot{\sigma}k_5}{\dot{\sigma}\cos^2 3\theta} + \frac{\ddot{\sigma}}{\dot{\sigma}}\tan 3\theta\begin{pmatrix} m_b\sigma_{ci}^{(1-\alpha)/\alpha}\left(\cos\theta - \frac{\sin\theta}{\sqrt{3}}\right) + \frac{1}{\alpha}(2\ddot{\sigma}\cos\theta)^{(1-\alpha)/\alpha}(2\cos\theta) \\ -\frac{(1-\alpha)\ddot{\sigma}}{\alpha^2}(2\sin\ \theta)^2(2\ddot{\sigma}\cos\theta)^{(1-2\alpha)/\alpha} \end{pmatrix} = M_4$$

$$\sin 3\theta = -\frac{3\sqrt{3}}{2}\frac{J_3}{\dot{\sigma}^3}$$

$$3\cos 3\theta\frac{\partial \theta}{\partial \boldsymbol{\sigma}} = -\frac{3\sqrt{3}}{2\dot{\sigma}^3}\left[\frac{\partial J_3}{\partial \boldsymbol{\sigma}} - \frac{3J_3}{\dot{\sigma}}\frac{\partial \dot{\sigma}}{\partial \boldsymbol{\sigma}}\right]$$

$$\frac{\partial \theta}{\partial \boldsymbol{\sigma}} = -\frac{\sqrt{3}}{2\cos 3\theta\dot{\sigma}^3}\left[\frac{\partial J_3}{\partial \boldsymbol{\sigma}} - \frac{3J_3}{\dot{\sigma}}\frac{\partial \dot{\sigma}}{\partial \boldsymbol{\sigma}}\right]$$

$$M_5 = -\frac{\sqrt{3}}{2\cos 3\theta\dot{\sigma}^3}$$

$$\frac{\partial C_2}{\partial \boldsymbol{\sigma}} = \frac{\partial C_2}{\partial \dot{\sigma}}\frac{\partial \dot{\sigma}}{\partial \boldsymbol{\sigma}} + \frac{\partial C_2}{\partial \theta}\frac{\partial \theta}{\partial \boldsymbol{\sigma}} = M_1\frac{\partial \dot{\sigma}}{\partial \boldsymbol{\sigma}} + M_4M_5\left[\frac{\partial J_3}{\partial \boldsymbol{\sigma}} - \frac{3J_3}{\dot{\sigma}}\frac{\partial \dot{\sigma}}{\partial \boldsymbol{\sigma}}\right]$$

$$\frac{\partial C_3}{\partial \boldsymbol{\sigma}} = \frac{\partial C_3}{\partial \dot{\sigma}}\frac{\partial \dot{\sigma}}{\partial \boldsymbol{\sigma}} + \frac{\partial C_3}{\partial \theta}\frac{\partial \theta}{\partial \boldsymbol{\sigma}} = M_2\frac{\partial \dot{\sigma}}{\partial \boldsymbol{\sigma}} + M_3M_5\left[\frac{\partial J_3}{\partial \boldsymbol{\sigma}} - \frac{3J_3}{\dot{\sigma}}\frac{\partial \dot{\sigma}}{\partial \boldsymbol{\sigma}}\right]$$

$$\frac{\partial^2 J_3}{\partial \boldsymbol{\sigma}^2} = \frac{1}{3}\begin{bmatrix} s_r - s_z - s_\theta & 2s_\theta & 2\tau_{rz} & 2s_z \\ 2s_\theta & s_z - s_r - s_\theta & 2\tau_{rz} & 2s_r \\ 2\tau_{rz} & 2\tau_{rz} & -6\tau_{rz} & -4\tau_{rz} \\ 2s_z & 2s_r & -4\tau_{rz} & s_\theta - s_z - s_r \end{bmatrix}$$

$$\frac{\partial^2 \dot{\sigma}}{\partial \boldsymbol{\sigma}^2} = \frac{1}{\dot{\sigma}}\left[0.5\frac{\partial \boldsymbol{s}}{\partial \boldsymbol{\sigma}} - \frac{\partial \dot{\sigma}}{\partial \boldsymbol{\sigma}}\otimes\frac{\partial \dot{\sigma}}{\partial \boldsymbol{\sigma}}\right]$$

$$\frac{\partial \boldsymbol{s}}{\partial \boldsymbol{\sigma}} = {}^1\!/_3\begin{bmatrix} 2 & -1 & 0 & -1 \\ -1 & 2 & 0 & -1 \\ 0 & 0 & 6 & 0 \\ -1 & -1 & 0 & 2 \end{bmatrix}; \frac{\partial \dot{\sigma}}{\partial \boldsymbol{\sigma}}\otimes\frac{\partial \dot{\sigma}}{\partial \boldsymbol{\sigma}} = \frac{1}{4\dot{\sigma}^2}\begin{bmatrix} s_r^2 & s_rs_z & 2\tau_{rz}s_r & s_rs_\theta \\ s_rs_z & s_z^2 & 2\tau_{rz}s_z & s_zs_\theta \\ 2\tau_{rz}s_r & 2\tau_{rz}s_z & 4\tau_{rz}^2 & 2\tau_{rz}s_\theta \\ s_rs_\theta & s_zs_\theta & 2\tau_{rz}s_\theta & s_\theta^2 \end{bmatrix}$$

$$\begin{aligned}\nabla^2 f &= \frac{\partial C_2}{\partial \boldsymbol{\sigma}}\frac{\partial \dot{\sigma}}{\partial \boldsymbol{\sigma}} + C_2\frac{\partial^2 \dot{\sigma}}{\partial \boldsymbol{\sigma}^2} + \frac{\partial C_3}{\partial \boldsymbol{\sigma}}\frac{\partial J_3}{\partial \boldsymbol{\sigma}} + C_3\frac{\partial^2 J_3}{\partial \boldsymbol{\sigma}^2} \\ &= \left(M_1\frac{\partial \dot{\sigma}}{\partial \boldsymbol{\sigma}} + M_4M_5\left[\frac{\partial J_3}{\partial \boldsymbol{\sigma}} - \frac{3J_3}{\dot{\sigma}}\frac{\partial \dot{\sigma}}{\partial \boldsymbol{\sigma}}\right]\right)\frac{\partial \dot{\sigma}}{\partial \boldsymbol{\sigma}} + C_2\frac{\partial^2 \dot{\sigma}}{\partial \boldsymbol{\sigma}^2} \\ &\quad + \left(M_2\frac{\partial \dot{\sigma}}{\partial \boldsymbol{\sigma}} + M_3M_5\left[\frac{\partial J_3}{\partial \boldsymbol{\sigma}} - \frac{3J_3}{\dot{\sigma}}\frac{\partial \dot{\sigma}}{\partial \boldsymbol{\sigma}}\right]\right)\frac{\partial J_3}{\partial \boldsymbol{\sigma}} + C_3\frac{\partial^2 J_3}{\partial \boldsymbol{\sigma}^2} \\ &= \left(M_1 - \frac{3J_3M_4M_5}{\dot{\sigma}}\right)\frac{\partial \dot{\sigma}}{\partial \boldsymbol{\sigma}}\otimes\frac{\partial \dot{\sigma}}{\partial \boldsymbol{\sigma}} + M_4M_5\frac{\partial J_3}{\partial \boldsymbol{\sigma}}\otimes\frac{\partial \dot{\sigma}}{\partial \boldsymbol{\sigma}} + C_2\frac{\partial^2 \dot{\sigma}}{\partial \boldsymbol{\sigma}^2} \\ &\quad + C_3\frac{\partial^2 J_3}{\partial \boldsymbol{\sigma}^2} + \left(M_2 - \frac{3J_3M_3M_5}{\dot{\sigma}}\right)\frac{\partial \dot{\sigma}}{\partial \boldsymbol{\sigma}}\otimes\frac{\partial J_3}{\partial \boldsymbol{\sigma}} + M_3M_5\frac{\partial J_3}{\partial \boldsymbol{\sigma}}\otimes\frac{\partial J_3}{\partial \boldsymbol{\sigma}}\end{aligned}$$

(ii) for $|\theta| \geq \theta_T$,

$$\frac{\partial C_1}{\partial \dot{\sigma}} = -1/3 m_b \sigma_{ci}^{(1-\alpha)/\alpha} R_2 \tan 3\theta_T + \frac{R_2 \sin 3\theta}{3\cos 3\theta_T} = S_1$$

$$\frac{\partial C_1}{\partial \theta} = \frac{k_2 m_b \sigma_{ci}^{(1-\alpha)/\alpha}}{\cos 3\theta_T} \cos 3\theta = S_2$$

$$\frac{\partial C_2}{\partial \sigma_m} = -\frac{\dot{\sigma}}{\ddot{\sigma}^2} m_b \sigma_{ci}^{(1-\alpha)/\alpha} \left(1 + \frac{k_2 \tan 3\theta_T}{3} - \frac{k_2 \sin 3\theta}{3\cos 3\theta_T}\right) - m_b \sigma_{ci}^{(1-\alpha)/\alpha} \left(\frac{\dot{\sigma}}{\ddot{\sigma}^2} + \left(k_2 \frac{\dot{\sigma}}{\ddot{\sigma}^2} + R_2\right)\left(\frac{\tan 3\theta_T}{3} - \frac{\sin 3\theta}{3\cos 3\theta_T}\right)\right) = S_3$$

$$\frac{\partial C_2}{\partial \dot{\sigma}} = -m_b \sigma_{ci}^{(1-\alpha)/\alpha} (A + B\sin 3\theta)\left(\frac{1}{\ddot{\sigma}} - \frac{\dot{\sigma}^2}{\ddot{\sigma}^3}\right) - \frac{\dot{\sigma}}{\ddot{\sigma}} 2 m_b \sigma_{ci}^{(1-\alpha)/\alpha} \left(R_3 + \frac{k_2 R_3 + k_3 R_2}{3\cos 3\theta_T}(\sin 3\theta_T - \sin 3\theta)\right) - m_b \sigma_{ci}^{(1-\alpha)/\alpha} \ddot{\sigma} \left(\frac{\partial R_3}{\partial \dot{\sigma}} + \frac{k_2 Y_3 + 2R_2 R_3 + k_3 Y_2}{3\cos 3\theta_T}(\sin 3\theta_T - \sin 3\theta)\right) = S_4$$

$$\frac{\partial R_1}{\partial \dot{\sigma}} = \frac{\dot{\sigma}^2}{\ddot{\sigma}^2} \frac{(1-\alpha)(1-2\alpha)}{\alpha^3} \left(4\cos^2 \theta_T\right)\left(2\ddot{\sigma}\cos\theta_T\right)^{(1-3\alpha)/\alpha} = Y_1$$

$$\frac{\partial R_2}{\partial \dot{\sigma}} = \frac{1}{P_2}\left(2R_1 \sin\theta_T \left(1 + \frac{\dot{\sigma}}{\ddot{\sigma}}\right) + m_b \sigma_{ci}^{(1-\alpha)/\alpha} \left(\frac{\cos\ \theta_T}{\sqrt{3}} + \langle\psi\rangle \sin\theta_T\right)\left(\frac{1}{\ddot{\sigma}} - \frac{\dot{\sigma}^2}{\ddot{\sigma}^3}\right) + 2Y_1 \ddot{\sigma} \sin\theta_T\right) - \frac{2\cos\theta_T}{P_2^2}\left(R_1 X_1 + R_1 T_1 + P_1 Y_1 + 4P_1 R_1^2 \cos\theta_T / P_2\right) = Y_2$$

$$\frac{\partial R_3}{\partial \dot{\sigma}} = \frac{s\sigma_{ci}^{1/\alpha} - m_b \sigma_{ci}^{(1-\alpha)/\alpha} \sigma_m}{m_b \sigma_{ci}^{(1-\alpha)/\alpha}} \left(\frac{1}{\ddot{\sigma}^3} - 3\frac{\dot{\sigma}^2}{\ddot{\sigma}^5}\right) = Y_3$$

$$\frac{\partial P_1}{\partial \dot{\sigma}} = 2R_1\, \ddot{\sigma} \sin\theta_T + m_b \sigma_{ci}^{(1-\alpha)/\alpha} \left(\frac{\cos\theta_T}{\sqrt{3}} + \langle\psi\rangle \sin\theta_T\right) \frac{\dot{\sigma}}{\ddot{\sigma}} + 2k_1 \sin\theta_T \frac{\dot{\sigma}}{\ddot{\sigma}} = T_1$$

$$X_1 = P_1 \frac{\dot{\sigma}}{\ddot{\sigma}^2} + (2R_1 \ddot{\sigma}\langle\psi\rangle \sin\theta_T)$$

$$\frac{\partial C_2}{\partial \theta} = -\frac{\dot{\sigma}}{\ddot{\sigma}}(3B\cos 3\theta) + m_b \sigma_{ci}^{\frac{1-\alpha}{\alpha}} \ddot{\sigma}(k_2 R_3 + k_3 R_2) \frac{\cos 3\theta}{\cos 3\theta_T} + 9Bm_b \sigma_{ci}^{\frac{1-\alpha}{\alpha}} \cos 3\theta \left(\frac{\ddot{\sigma}}{\ddot{\sigma}}\right) = S_5$$

$$\frac{\partial C_3}{\partial \sigma_m} = \frac{k_2\sqrt{3}}{2\dot{\sigma}^3 \cos 3\theta_T} m_b \sigma_{ci}^{\frac{1-\alpha}{\alpha}} = S_6$$

$$\frac{\partial C_3}{\partial \dot{\sigma}} = \frac{3\sqrt{3}}{2} m_b \sigma_{ci}^{\frac{1-\alpha}{\alpha}} \left(\frac{\ddot{\sigma}(k_2 R_3 + k_3 R_2)}{3\dot{\sigma}^3 \cos 3\theta_T} - \frac{B}{\dot{\sigma}^2 \ddot{\sigma}} + \frac{3B}{\ddot{\sigma}^4}\right) = S_7$$

$$\begin{aligned}
\nabla^2 f &= \frac{\partial C_1}{\partial \boldsymbol{\sigma}}\frac{\partial \dot{\sigma}}{\partial \boldsymbol{\sigma}} + \frac{\partial C_2}{\partial \boldsymbol{\sigma}}\frac{\partial \dot{\sigma}}{\partial \boldsymbol{\sigma}} + C_2 \frac{\partial^2 \dot{\sigma}}{\partial \boldsymbol{\sigma}^2} + \frac{\partial C_3}{\partial \boldsymbol{\sigma}}\frac{\partial J_3}{\partial \boldsymbol{\sigma}} + C_3 \frac{\partial^2 J_3}{\partial \boldsymbol{\sigma}^2} \\
&= \left(\frac{\partial C_1}{\partial \dot{\sigma}}\frac{\partial \dot{\sigma}}{\partial \boldsymbol{\sigma}} + \frac{\partial C_1}{\partial \theta}\frac{\partial \theta}{\partial \boldsymbol{\sigma}}\right)\frac{\partial \sigma_m}{\partial \boldsymbol{\sigma}} + \left(\frac{\partial C_2}{\partial \sigma_m}\frac{\partial \sigma_m}{\partial \boldsymbol{\sigma}} + \frac{\partial C_2}{\partial \dot{\sigma}}\frac{\partial \dot{\sigma}}{\partial \boldsymbol{\sigma}} + \frac{\partial C_2}{\partial \theta}\frac{\partial \theta}{\partial \boldsymbol{\sigma}}\right)\frac{\partial \dot{\sigma}}{\partial \boldsymbol{\sigma}} \\
&\quad + C_2 \frac{\partial^2 \dot{\sigma}}{\partial \boldsymbol{\sigma}^2} + C_3 \frac{\partial^2 J_3}{\partial \boldsymbol{\sigma}^2} + \left(\frac{\partial C_3}{\partial \sigma_m}\frac{\partial \sigma_m}{\partial \boldsymbol{\sigma}} + \frac{\partial C_3}{\partial \dot{\sigma}}\frac{\partial \dot{\sigma}}{\partial \boldsymbol{\sigma}}\right)\frac{\partial J_3}{\partial \boldsymbol{\sigma}} \\
&= S_1 \left(\frac{\partial \dot{\sigma}}{\partial \boldsymbol{\sigma}} \otimes \frac{\partial \sigma_m}{\partial \boldsymbol{\sigma}}\right) + S_2 X_2 \left(\frac{\partial J_3}{\partial \boldsymbol{\sigma}} \otimes \frac{\partial \sigma_m}{\partial \boldsymbol{\sigma}}\right) + S_3 \left(\frac{\partial \sigma_m}{\partial \boldsymbol{\sigma}} \otimes \frac{\partial \dot{\sigma}}{\partial \boldsymbol{\sigma}}\right) + C_2 \frac{\partial^2 \dot{\sigma}}{\partial \boldsymbol{\sigma}^2} \\
&\quad + C_3 \frac{\partial^2 J_3}{\partial \boldsymbol{\sigma}^2} + \left(S_4 - \frac{3X_2 J_3}{\dot{\sigma}}(S_2 + S_5)\right) + S_5 X_2 \left(\frac{\partial \dot{\sigma}}{\partial \boldsymbol{\sigma}} \otimes \frac{\partial J_3}{\partial \boldsymbol{\sigma}}\right) \\
&\quad + S_6 \left(\frac{\partial \sigma_m}{\partial \boldsymbol{\sigma}} \otimes \frac{\partial J_3}{\partial \boldsymbol{\sigma}}\right) + S_7 \left(\frac{\partial \dot{\sigma}}{\partial \boldsymbol{\sigma}} \otimes \frac{\partial J_3}{\partial \boldsymbol{\sigma}}\right)
\end{aligned}$$